

Effects of Sb substitution on structural and superconducting properties of Bi in $\text{Bi}_{1.75-x}\text{Pb}_{0.25}\text{Sb}_x\text{Sr}_2\text{Ca}_2\text{Cu}_3\text{O}_y$ superconductor

Ebru Kış Çam¹ · Kemal Kocabaş¹

Received: 4 March 2016 / Accepted: 22 April 2016 / Published online: 27 April 2016
© Springer Science+Business Media New York 2016

Abstract In this work, we investigate the effects of Sb substitution on structural and superconducting properties of $\text{Bi}_{1.75-x}\text{Pb}_{0.25}\text{Sb}_x\text{Sr}_2\text{Ca}_2\text{Cu}_3\text{O}_y$ superconductor for $x = 0.00\text{--}0.20$. Powder X-ray diffraction analysis showed that the samples consist of the Bi-2212 phase is dominant in all samples and the impurity phases was observed to increase with increasing the substitution ratio. Moreover, the intensity of the (115) peak for the low phase and the (117) peak of the high temperature phase decrease with increasing Sb substitution. The grain size, grain connectivity and surface morphology of the samples are identified from SEM microphotographs. Temperature dependence of resistivity revealed the highest T_c value at 110 K for $x = 0.1$ Sb substitution ratio. The density of all prepared samples were determined and was found to decrease with increasing Sb substitution, while porosity found to increase with increasing the substitution ratio.

1 Introduction

Bi-Sr-Cu-O a novel family of superconducting oxides was investigated by Mitchell et al. [1]. BSCCO(Bi-Sr-Ca-Cu-O) was discovered as a new class of superconductor by adding Ca in Bi-Sr-Cu-O system [2]. Then after discovery of high-temperature superconductors of BSCCO general formula of this system was obtained as $\text{Bi}_2\text{Sr}_2\text{Ca}_{n-1}\text{Cu}_n\text{O}_{4+2n+x}$ ($n = 1, 2$ and 3). These three phases (Bi-2201, Bi-2212 and Bi-2223) have one, two and three Cu-O layers

hence different T_c can be formed as 20, 85 and 110 K respectively [3, 4]. It is very difficult to obtain the pure monophasic $\text{Bi}_2\text{Sr}_2\text{Ca}_2\text{Cu}_3\text{O}_{10}$ (2223) material with the highest T_c because of the existence of three or more phases having a similar layered structure. Defects occur during synthesis and it becomes difficult to isolate a single superconducting phase.

In high- T_c superconductors, understanding the role of substitutes and dopants is of great importance for scientific and applied purposes. Properties of Bi-based superconductors can be controlled by substitution with elements that have different ionic radius and binding characteristics. Since Maeda et al. [2] discovered superconductivity in the Bi-2223 system, a large number of researchers have been focused on the synthesis and the use of various dopants to increase the T_c of these ceramics in addition to increasing the volume fraction of the high- T_c phase in multiphase ceramics.

Pb has been found to be one of the most effective elements for the 110 K phase formation [5–11]. For example, partial substitution of Pb in Bi-based system raised the critical temperature [12, 13]. Pb addition results showed the optimal Pb amount lies 0.3 and 0.4 [14, 15]. So when discussing Bi-system there are two different composing referred as BSCCO and BPSCCO. The new phase of monoclinic system known as 4441 phase with the highest T_c in Bi-based system was found at 140 K [16]. Substitution of BPSCCO system with different elements has been studied to be useful and productive in improving the properties of high- T_c superconductors [17–27]. In a recent work, the effect of YBCO addition on the BPSCCO system was investigated [28].

The effect of Sb substitution on critical temperatures with or without Pb of Bi-based superconductors has not been understood yet or clarified. Many studies of Sb

✉ Ebru Kış Çam
ebru.kis@deu.edu.tr

¹ Department of Physics, Dokuz Eylül University, 35160 Izmir, Turkey

substitution into Bi-based superconductor have been made to understand the effects on their superconducting, magnetic and mechanical properties [29–40]. Partial substitutions of bismuth by Sb and Pb have been reported to cause improvements in the superconducting properties [34]. Hangbao et al. [29] determined a $T_{c;\text{onset}}$ of 120 K and $T_{c;\text{offset}}$ of 92 K when doped Sb alone in the $\text{Bi}_{2-x}\text{Sb}_x\text{Sr}_2\text{Ca}_2\text{Cu}_3\text{O}_y$ ceramics and a T_c of 132 K for $\text{Bi}_{1.9}\text{Pb}_x\text{Sb}_{0.1}\text{Ca}_2\text{Cu}_3\text{O}_y$ ceramics prepared by the conventional ceramic method [30]. The partial replacement of Sb in Bi site has increased the T_c onset up to 135 K [31]. Studies indicate that ceramics which are a mixture of low and high T_c phases are formed by substitution with Pb or Pb and Sb together. Partial replacement of Bi by Pb and Sb produces materials of extremely high phase purity, and antimony plays an important role in accelerating the formation of the phase with higher superconductive transition in the Bi-2223 system. The existence of Sb is thought to make the system more reactive, promotes the kinetics of the reaction and therefore elevates the high T_c phase and Sb has been stated to be effective in preventing Pb from evaporating during calcinations in BSCCO system [21]. It is well known that the length of c-parameter plays an important role in order to enhance the superconducting properties was found to decrease and hence contract the volume of unit cell as the content of Sb increased [39]. The ionic radii of Bi, Pb and Sb are 1.03, 1.19 and 0.76 Å, respectively.

Substituting of antimony applies a stabilizing effect on the formation of Bi-2223 high T_c phase. However, the effect of the substitutions on synthesis processes and on final superconducting characteristics could depend on the type and phase content of the precursor powders, technological method and on the type of the substituent. Briefly, it could depend on when and how the dopant is added to a certain composition.

In previous works in our group, we interested in substitution of antimony in Bi-based systems [37, 40]. In [37], the effect of partial substitution of Cu in $\text{Bi}_{1.7}\text{Pb}_{0.3}\text{Sr}_2\text{Ca}_2\text{Cu}_{3-x}\text{Sb}_x\text{O}_y$ at $x = 0.00, 0.05, 0.10, 0.15,$ and 0.20 levels on the electrical and structural properties was investigated and substitution of Cu partially by Sb in $\text{Bi}_{1.7}\text{Pb}_{0.3}\text{Sr}_2\text{Ca}_2\text{Cu}_{3-x}\text{Sb}_x\text{O}_y$ superconductors resulted in the formation of a phase commonly known as 4441 phase. In [40], the effect of sintering temperature in $\text{Bi}_{1.7}\text{Pb}_{0.2}\text{Sb}_{0.1}\text{Sr}_2\text{Ca}_2\text{Cu}_3\text{O}_y$ was investigated and it determined that 845°C can be taken as the optimal temperature.

In this study, the effect of Sb addition on both superconducting and structural properties of BPSCCO ceramics has been investigated. In addition, for identification of the superconducting and non-superconducting phases, X-ray powder diffraction analysis (XRD) was used. Furthermore, scanning electron microscopy (SEM) was employed to

investigate the surface microstructure and surface morphology of the samples considered.

2 Experimental details

The ceramic superconducting samples of $\text{Bi}_{1.75-x}\text{Pb}_{0.25}\text{Sb}_x\text{Sr}_2\text{Ca}_2\text{Cu}_3\text{O}_y$ system were prepared from appropriate mixtures of high purity (Aldrich Chem. Co. 99.9 %) $\text{Bi}_2\text{O}_3,$ $\text{PbO}, \text{Sb}_2\text{O}_3, \text{SrCO}_3, \text{CaCO}_3$ and CuO by standard solid state reaction method.

The substitution ratios of Bi by Sb are in $x = 0.00\text{--}0.20$ range. First starting component powders have been weighted in cationic ratios with ± 0.0001 g sensitivity Scaltex balance. After weighting, powders were mixed and well grounded at five different ratios by naming A($x = 0.00$), B($x = 0.05$), C($x = 0.10$), D($x = 0.15$), E($x = 0.20$). These mixtures heat-treated powders were grounded twice at 800°C for 20 h in alumina crucibles in a furnace (Nabatherm) in air atmosphere initially. The heat-treated powders were grounded again in a mortar with a pestle and were uniaxially pressed at 450 MPa pressure. Prepared pellets were 13 mm in diameter and 1.5–2 mm thick. The sintering condition such as temperature, time, atmosphere and cooling rate a very important role in obtaining good high- T_c superconducting materials and BSCCO system has been found to required a long sintering time [4]. The sintering temperature is commonly in the $845\text{--}855^\circ\text{C}$ range [41, 42]. In previous work, the effect of sintering temperature in $\text{Bi}_{1.7}\text{Pb}_{0.2}\text{Sb}_{0.1}\text{Sr}_2\text{Ca}_2\text{Cu}_3\text{O}_y$ was investigated and it determined that 845°C can be taken as the optimal temperature [40]. So the pellets were sintered in a Protherm tube furnace at 850°C for 150 h by using furnace cooled down to room temperature.

Resistances of all samples were measured as a function of temperature using the dc four-point probe technique in Oxford Cyropump system. X-ray diffraction (XRD) patterns of Sb substituted samples were obtained by Philips Xpert Pro Diffractometer in the $2\theta = 3^\circ\text{--}60^\circ$ range with $\text{CuK}\alpha$ radiation. In order to calculate the lattice parameters (a, b, c), XRD results were analyzed using Powder Diffraction Programme (PDP). The grain size, grain connectivity and surface morphology of the samples are identified SEM microphotographs. Scanning electron microscopy (SEM) images were taken by using a Philips XL 30S FEG SEM to understand the microstructure. The elemental compositions and impurities in different regions of the samples were analyzed by EDAX using the same system. Finally, the bulk densities were obtained from an Archimedes water displacement technique with a density measurement kit (Sartorius). The porosity was calculated from these density results.

3 Results and discussions

3.1 Resistivity measurements

Variation of resistance with the temperature are shown for all samples in Fig. 1 in $T = 50\text{--}300$ K range. All samples display a metallic character above onset temperature which is defined as the temperature where resistance–temperature plot deviates from linearity. The onset temperature was measured as 108 K for the undoped sample A and 106 K for sample B ($x = 0.05$). It was observed that sample C ($x = 0.10$) has the highest onset temperature as 110 K

among all samples. The onset temperature decreases to 107 K for sample D ($x = 0.15$) and 104 K for sample E ($x = 0.2$). The similar behavior for the onset temperature is observed for T_c , is described as the temperature where the resistance is zero, too. This reduction is related to the increase of the Bi-2212 phase formation. The critical temperatures were determined as 87, 75, 87, 86 and 47 K for samples A, B, C, D and E, respectively. Onset temperatures were plotted versus Sb substitutional ratio (x) in Fig. 2. Critical temperature was affected negatively by high increasing of x ratio such as $x = 0.20$ seen Fig. 2. This may be an indication of increasing of impurities phase

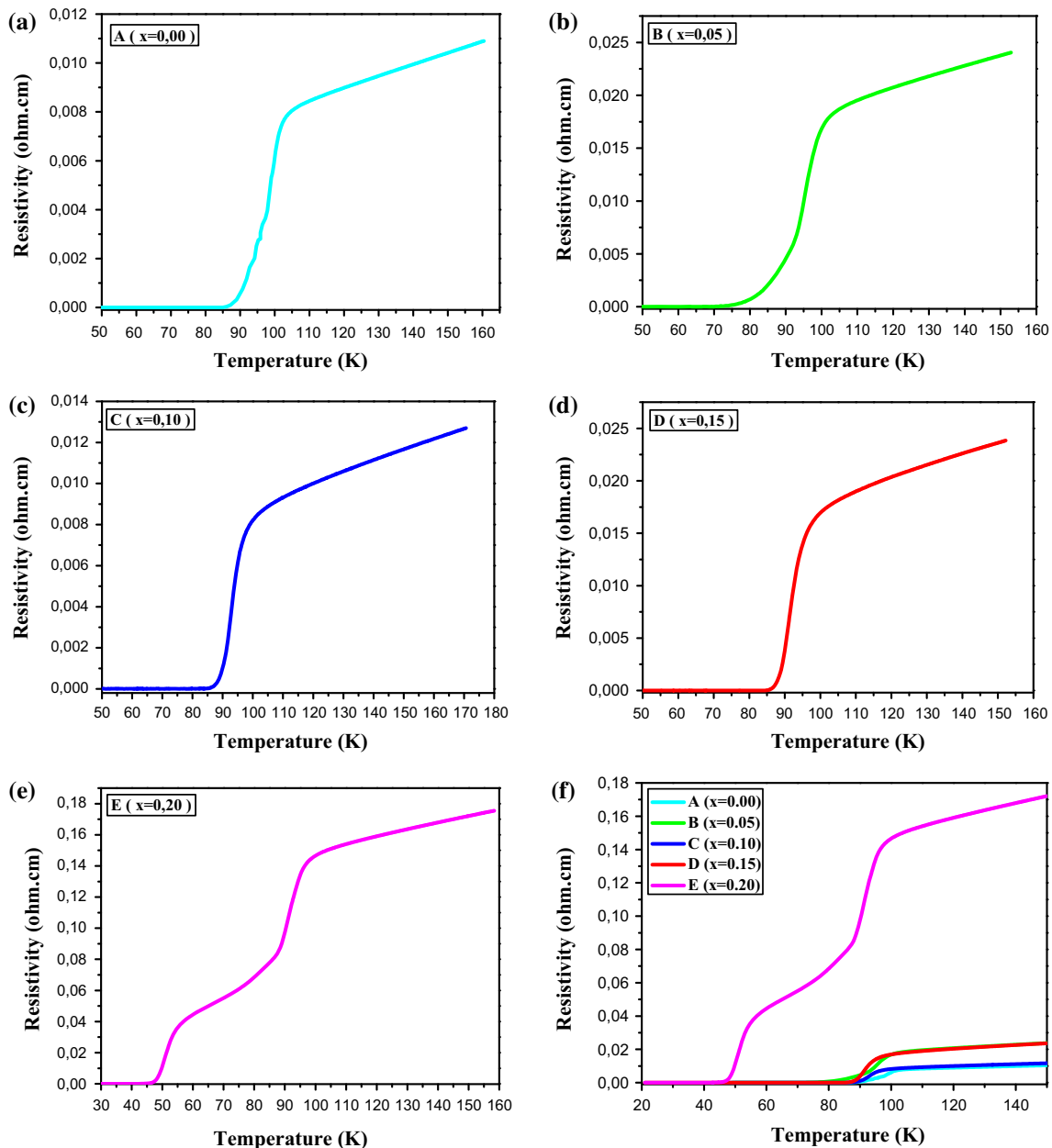


Fig. 1 Resistance–temperature plots in all samples [A($x = 0.00$), B($x = 0.05$), C($x = 0.10$), D($x = 0.15$), E($x = 0.20$)]

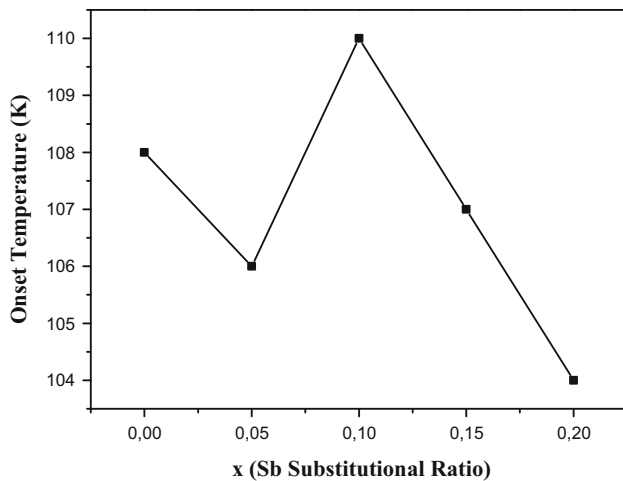


Fig. 2 Variation of onset temperature with x substitutional ratio

or decreasing of the high temperature phase by increasing the substitutional ratio. This idea is also supported by the XRD patterns.

Another characteristic of superconductivity is the transition temperature width, is a parameter of the phase purity, defined as $\Delta T_c = T_{c;onset} - T_{c;offset}$. The transition temperatures of the samples were 21, 31, 23, 21 and 57 K, respectively. The variation of ΔT with x ratio is further plotted in Fig. 3. As seen in Figs. 2 and 3, ΔT has minimum value and maximum onset temperature in sample C ($x = 0.10$). On the contrary, sample E doped with maximum antimony has the maximum ΔT and the minimum onset temperature. Thus it can be said that optimum Sb ratio for T_c is seen in the sample doped Sb with $x = 0.10$. Therefore it may be proven that the onset temperature and transition temperature are closely related. As shown in Figs. 2 and 3, an increase of the onset temperature reduces ΔT . Table 1 shows these results.

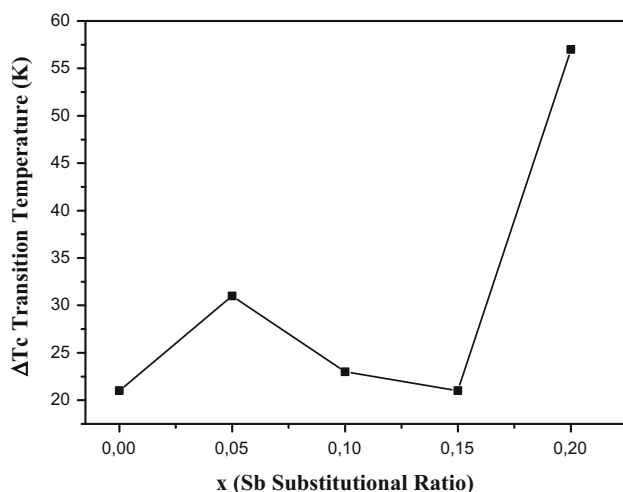


Fig. 3 Variation of transition temperature with x substitutional ratio

3.2 XRD measurements

XRD powder patterns of the samples are shown in Fig. 4. The high- T_c and low- T_c phase peaks were determined by using the tables given in [43, 44]. All samples have multiphase nature with high temperature and low temperature peaks. Patterns obtained from XRD measurements provide a knowledge not only for superconducting phases but also on undesired impurity phases. It is observed that Bi-2212 phase is dominant in all samples. An increase in impurity phases was observed by increasing substitutional ratio. The number of impurity phases and intensities of these phases was increased with Sb substitution. Intensity of high- T_c , low- T_c peaks and peaks of impurity phases were closer in E sample doped with maximum Sb as seen Fig. 4. This may be reason for the transition step in the resistance–temperature curve. The Bi-2223 peaks are presented by H(hkl) Miller indices while the peaks of Bi-2212 phase are described by L(hkl) Miller indices in the diagrams. The characteristic L(002) and H(002) peaks in BSCCO system were observed in all samples with different intensities. L(002) peak is evident only A and D samples.

The intensities of the most obvious peak observed in all samples is the L (115) peak in $2\theta = 27.5^\circ$. Intensity of this peak with the variation of substitutional ratio is plotted in Fig. 5. It was observed that this graphic is in harmony with the Fig. 2. This may be an indication that these peaks have significant effects on the onset temperature. In addition reduction in the intensity of peaks L(117) in $2\theta = 31.1^\circ$, L(200) in $2\theta = 33.1^\circ$, H(1111) in $2\theta = 35.5^\circ$ and an increasing of peak H(119) in $2\theta = 31.9^\circ$ were observed by increasing of substitutional ratio.

We observed that the most significant peaks in high- T_c phase is H (117) peak at $2\theta = 28.8^\circ$. Variation of this peak intensity with substitutional ratio is shown in Fig. 6. Figure 6 has a good agreement with Fig. 5. We can conclude that increasing substitutional ratio causes the same effect accordingly, in these two distinct peaks. By using of the peaks in the XRD patterns in all samples a, b, c lattice parameters were calculated which given in Table 2. All the samples remain in tetragonal structure which is $a = b \neq c$. The results we obtained and theoretical results of Bi-2223 system ($a = b = 5.4 \text{ \AA}$; $c = 37 \text{ \AA}$) are in well agreement. For 2223 high T_c phase, a comparison of these values shows that an increase in cell parameters in a and b directions while decrease in c direction occurs in sample C. In [39] the length of c-lattice that plays an important role of superconducting properties was found to decrease and hence contract the volume of unit cell as the content of Sb increased. According to our study, the XRD pattern of 2212 low- T_c phase is marked. That's why low- T_c must be calculated in the lattice parameters obtained from the peak. It was calculated and

Table 1 The critical temperatures, resistivity and density of the samples $\text{Bi}_{1.75-x}\text{Pb}_{0.25}\text{Sb}_x\text{Sr}_2\text{Ca}_2\text{Cu}_3\text{O}_y$

x (substitutional ratio)	$T_{c,\text{onset}}$ (K)	$T_{c,\text{offset}}$	ΔT_c (K)	R (120 K) m Ω	ρ (g/cm ³)
A (x = 0.00)	108	87	21	8.98	5.8946
B (x = 0.05)	106	75	31	20.80	5.6491
C (x = 0.10)	110	87	23	9.91	5.4878
D (x = 0.15)	107	86	21	20.33	5.4171
E (x = 0.20)	108	87	21	8.98	5.5076

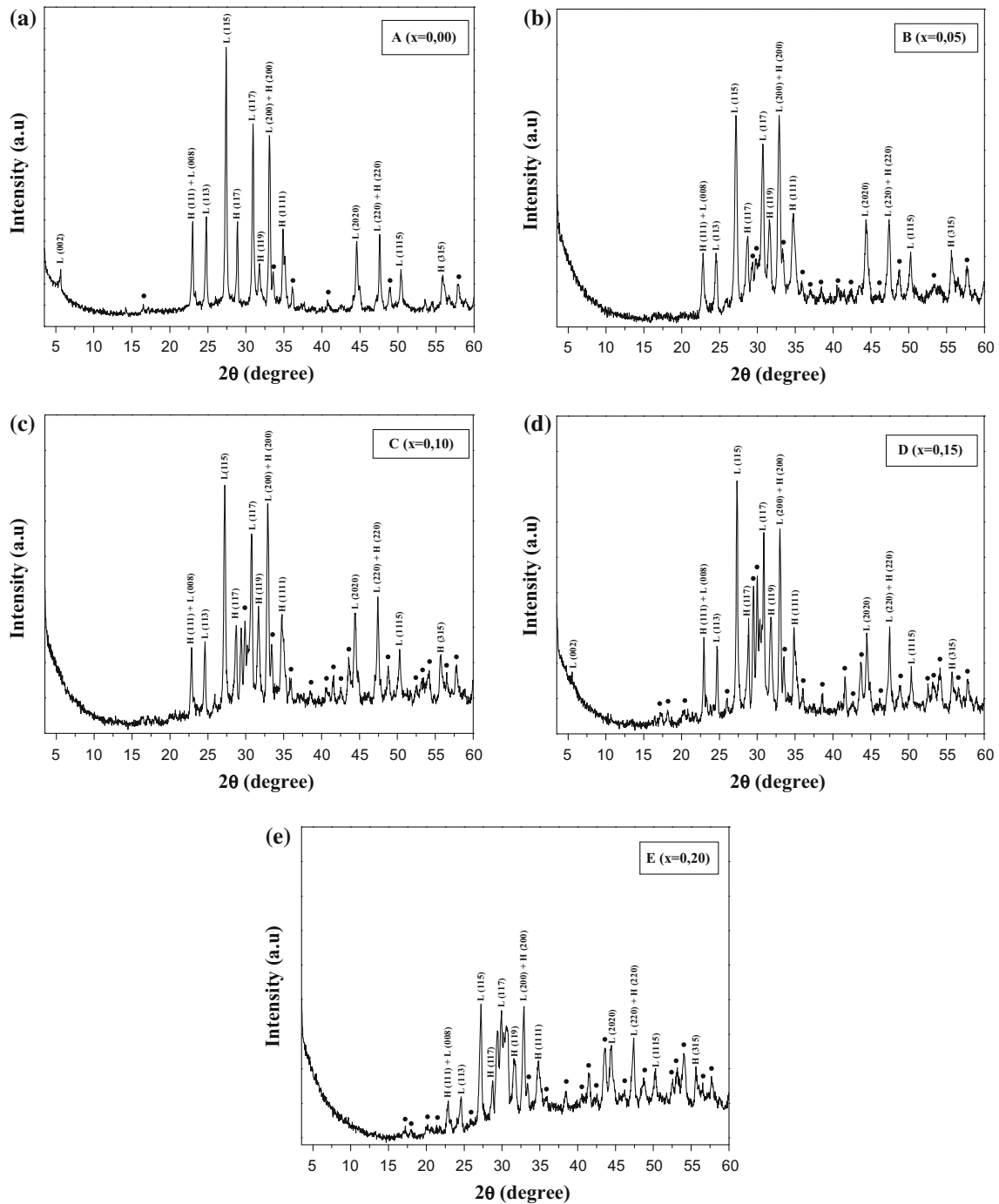


Fig. 4 XRD patterns for $\text{Bi}_{1.75-x}\text{Pb}_{0.25}\text{Sb}_x\text{Sr}_2\text{Ca}_2\text{Cu}_3\text{O}_y$ ($0; 00 \leq x \leq 0; 20$) samples respectively. (• show impurity phases)

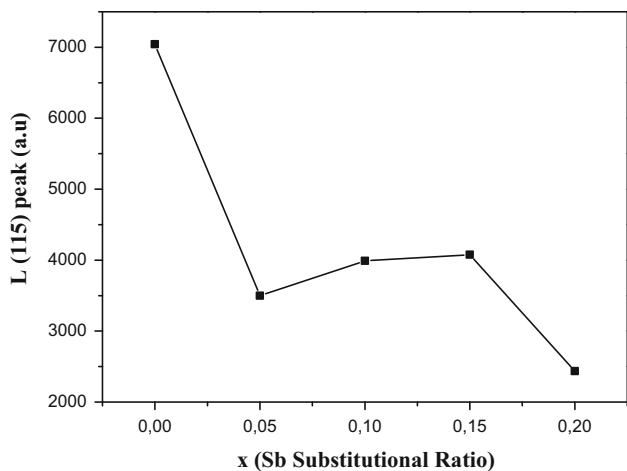


Fig. 5 Variation of L(115) peak with x substitutional ratio

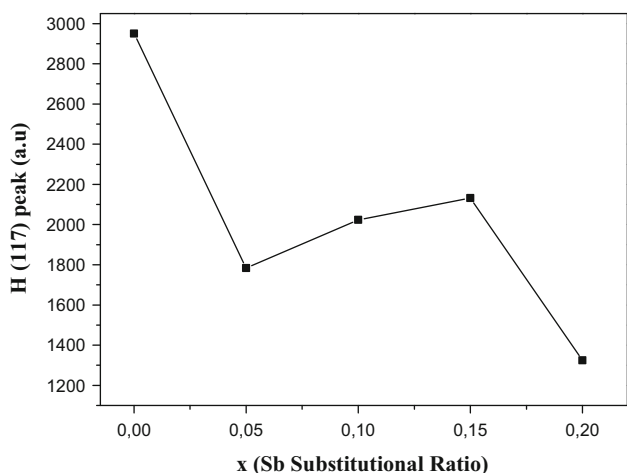


Fig. 6 Variation of H(117) peak with x substitutional ratio

given in Table 3. These results ensure compliance with the theoretical results of the Bi-2212 system.

3.3 SEM and EDAX analysis

The most important reason of high transition temperature and low critical current density in ceramic superconductors is granular structures. The microstructures of the top surfaces of all samples are shown in SEM photographs taken at different magnification in Figs. 7, 8, 9, 10 and 11. As it

can be seen from the photos, the most prominent of the fundamental properties of ceramic superconductors is granular structure. All particles are randomly oriented and grain boundaries in the samples appears in contact with each other to form weak bonds. This is one of the characteristics of high-temperature superconductors.

Sample A and B have fine crystalline and homogeneous structure. Shape of grains is plate-like for these samples. The occurrence of grains with plate-like structure is a signature of the Bi-2223 phase formation. Plate-like and needle-like forms are observed in other samples C, D and E together. With increasing substitutional ratio, the grain size decreasing and grain structure was broken down. For example, the grain size in undoped sample A is approximately 15 μm and in sample E which has maximum substitutional ratio is 6 μm. In B sample with x = 0.05 substitutional ratio approximately 27 μm needle-like form was observed as seen Fig. 8.

In addition, from EDAX analysis, we investigate weight ratios of elements in various regions of samples as seen in Figs. 12, 13, 14, 15 and 16. According to these results, weight ratios of all elements are different in various regions of the same sample. For instance, while ratios of O, Cu, Sr, Ca, Pb, Bi of a specified region in sample A are 5.01, 1.37, 9.88, 0.28, 25.84, 57.62, the same ratios in another region in the same sample are determined as 9.06, 4.70, 16.34, 0.22, 0.00, 69.68 respectively. As can be seen from these results, two-fold ratios in O, Cu and Sr was observed between the regions and Pb was observed as 25.84 in specified region whereas there was no Pb in another region. This shows that different phases was formed in different regions and general structure is not homogeneous. Among the doped samples, sample C has maximum oxygen content. Also sample C has highest critical temperature in doped sample. It is believed that the relationship oxygen content and superconductivity in the Bi-2223 compound can only be correctly established when there is a clear understanding on the behavior of the lead ion [39].

3.4 Density measurements

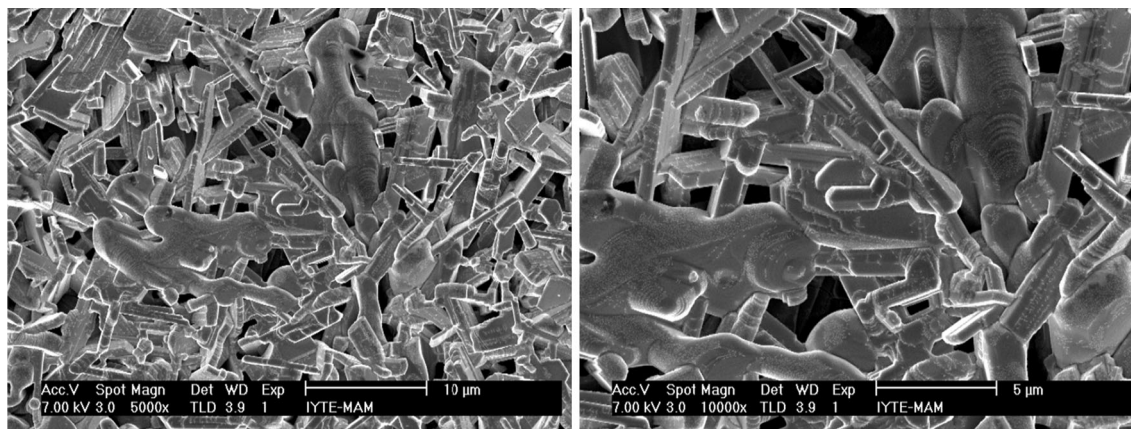
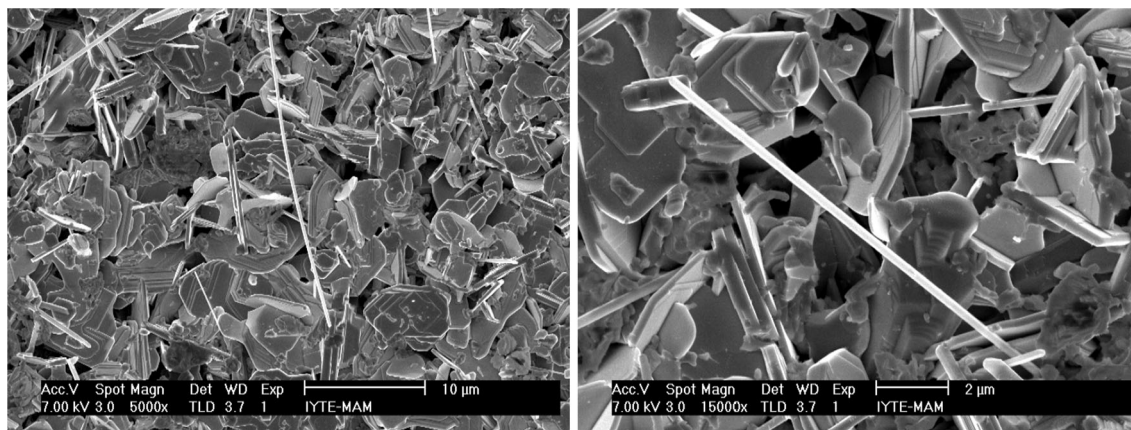
Densities of samples prepared with different antimony concentrations were determined from Archimedes' principle by given the following equation.

Table 2 Lattice parameters obtained from peaks of 2223 high-Tc phase in all samples

x (substitutional ratio)	V (cm ³)	A = b (Å)	C (Å)	α = β = γ
A (x = 0.00)	1082.9390	5.4079	37.0284	90
B (x = 0.05)	1082.7420	5.4074	37.0291	90
C (x = 0.10)	1082.9390	5.4079	37.0284	90
D (x = 0.15)	1082.7420	5.4074	37.0291	90
E (x = 0.20)	1082.7430	5.4074	37.0293	90

Table 3 Lattice parameters obtained from peaks of 2212 low-Tc phase in all samples

x (substitutional ratio)	V (cm ³)	A = b (Å)	C (Å)	$\alpha = \beta = \gamma$
A (x = 0.00)	889.1041	5.4079	30.4019	90
B (x = 0.05)	889.0504	5.4079	30.3995	90
C (x = 0.10)	889.0504	5.4079	30.3995	90
D (x = 0.15)	889.1473	5.4079	30.4025	90
E (x = 0.20)	889.0504	5.4079	30.3995	90

**Fig. 7** SEM photographs with different size for sample A**Fig. 8** SEM photographs with different size for sample B

$$\rho = \frac{W(h)[\rho(s) - \rho(h)]}{0.99983[W(s) - W(h)]} + \rho(h) \quad \rho(h) = 0.0012 \text{ g/cm}^3$$

where $\rho(h)$, $\rho(s)$, $W(h)$, $W(s)$ are densities of air and pure water and their weights in medium, respectively. The densities of samples were determined by Archimedes water displacement method. Densities of pellets obtained by using this method are given in Table 1. The densities of pellets were calculated to be 4.1947, 3.67212, 3.8082, 3.3670 and 3.7214 g/cm³ in A to E samples respectively from dimensional measurements. The theoretical density of

Bi_{2-x}Pb_xSr₂Ca₂Cu₃O_y sample was obtained from lattice parameters as 6.313 g/cm³ [45]. Density for Sb and Pb-doped BSCCO ceramics was calculated as 6.2 g/cm³ [16]. Bulk density of BSCCO pellet with Pb-doped was obtained using theoretical density of 6.45 g/cm³ [46]. The obtained results by water displacement technique are in the 86–94 % range of theoretical density, which is calculated from the lattice parameters to be 6.3 g/cm³. Figure 17 indicates density varies with the substitutional ratio.

Bi_{2-x}Pb_xSr₂Ca₂Cu₃O_y sample was produced in another study with similar methods in our study for x = 0.25

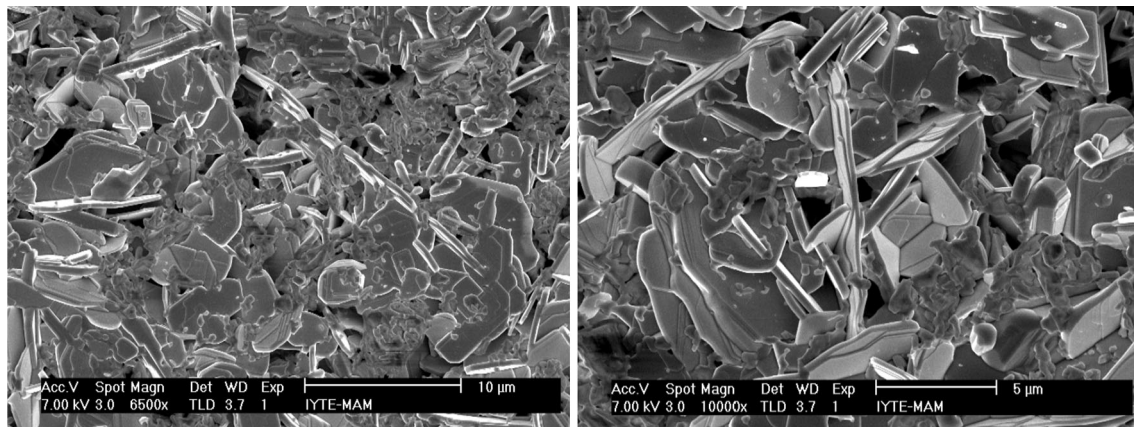


Fig. 9 SEM photographs with different size for sample C

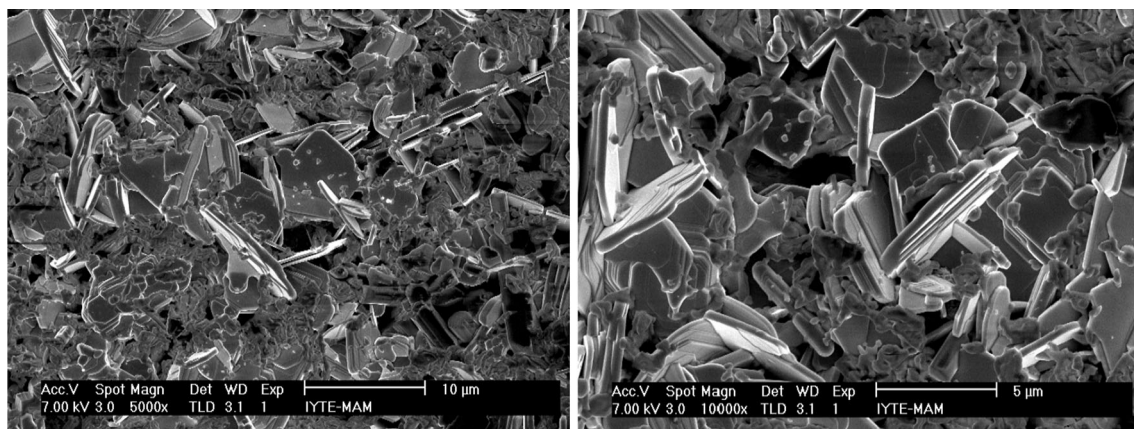


Fig. 10 SEM photographs with different size for sample D

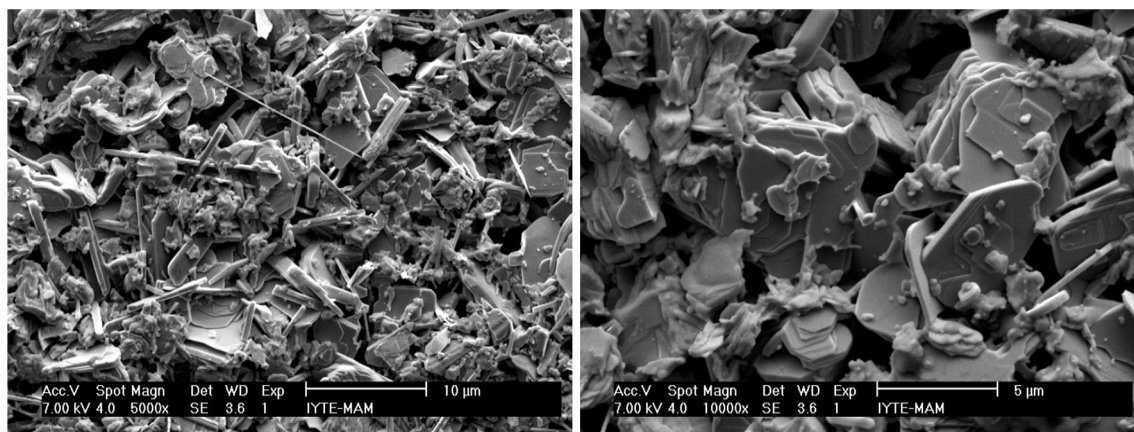


Fig. 11 SEM photographs with different size for sample E

for (in this case with the same formula as in our A sample) the onset and critical temperatures obtained as 118, 108 K respectively. In [47], it is clearly observed a decrease in porosity by increasing of Pb concentrations up to 0.3 when variation of porosity with Pb concentrations examined. This

behavior is due to the increasing of connection between the superconducting grains. Excess of lead content ($0.3 < x$) may cause a decrease of contact in the region between this grains and cavities are formed, as a result. Smaller density remarks the presence of pores between grains in the structure

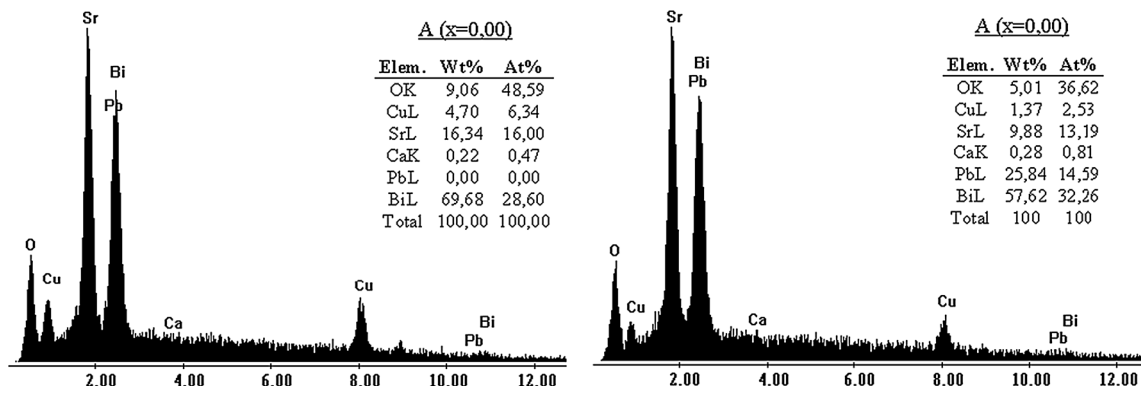


Fig. 12 EDAX analysis results relating to different areas for sample A

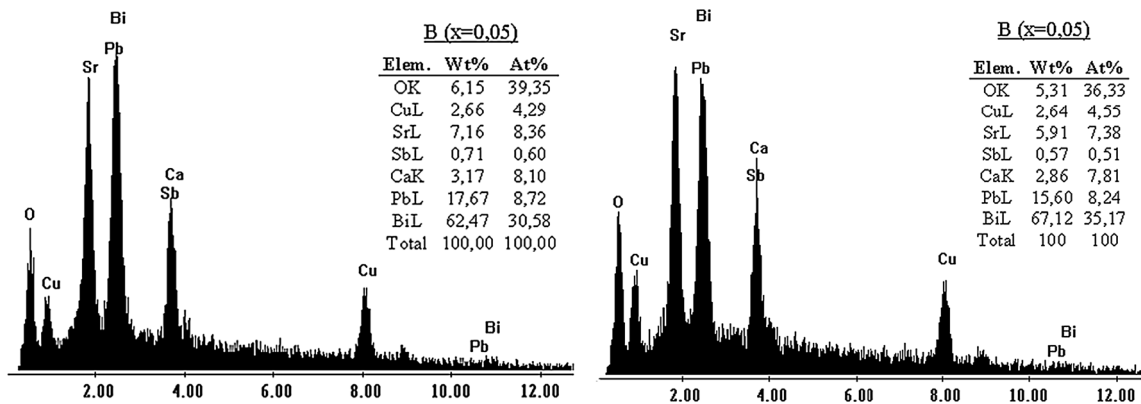


Fig. 13 EDAX analysis results relating to different areas for sample B

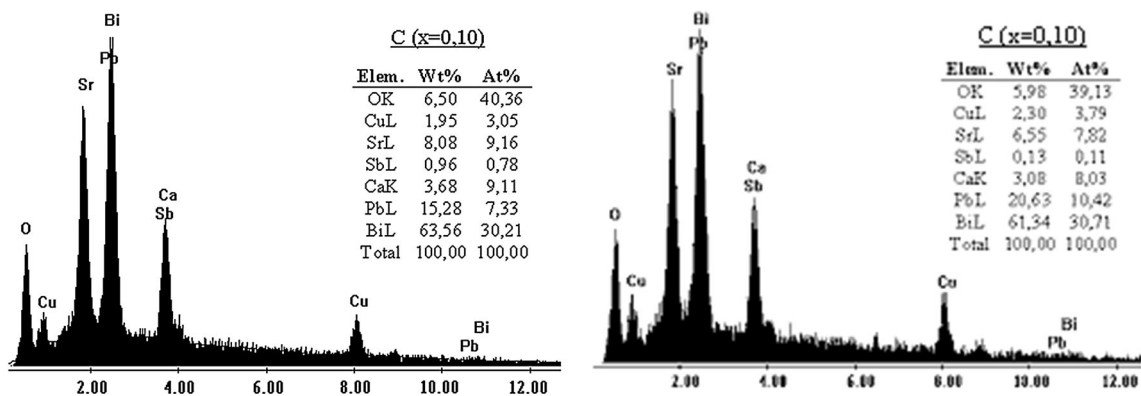


Fig. 14 EDAX analysis results relating to different areas for sample C

which affects T_c values negatively. Most open pore volume was occupied by water during tests. By taking theoretical densities taken as 6.3 g/cm^3 , pellets have 33–46 % porosity. Figure 18 shows substitutional ratio versus the porosity. It can be seen that sample C has minimum porosity in doped

sample. Also sample C has highest critical temperature in doped sample. This graph is compatible with Fig. 3 which shows variation of transition temperature with substitutional ratio. This is an indication that porosity of samples affect on transition temperature.

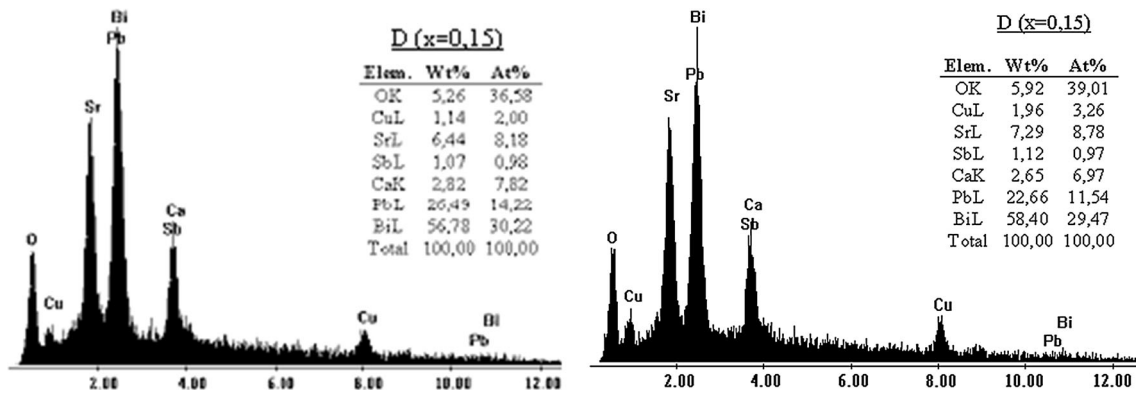


Fig. 15 EDAX analysis results relating to different areas for sample D

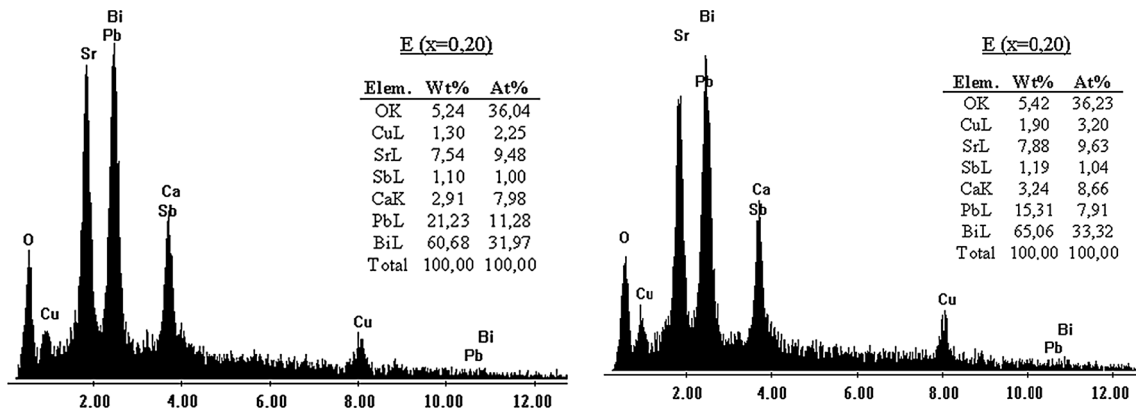


Fig. 16 EDAX analysis results relating to different areas for sample E

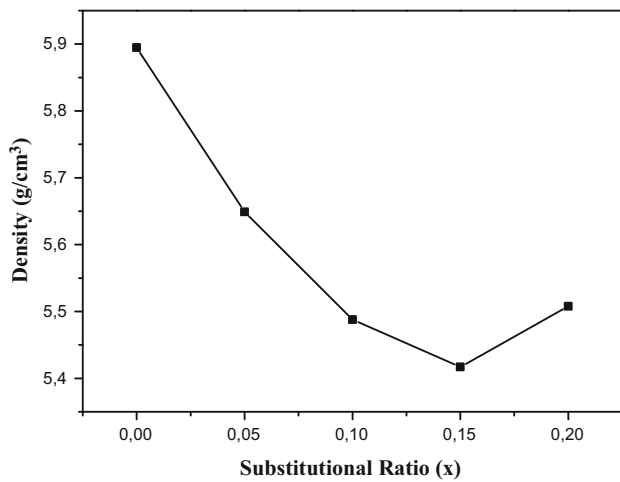


Fig. 17 Variation of densities with x substitutional ratio in $\text{Bi}_{1,75-x}\text{Pb}_{0,25}\text{Sb}_x\text{Sr}_2\text{Ca}_2\text{Cu}_3\text{O}_y$ ($0.00 \leq x \leq 0.20$) system

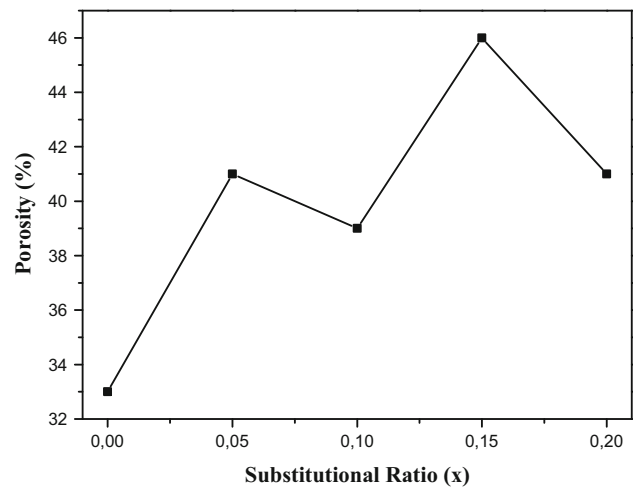


Fig. 18 Variation of porosity with x substitutional ratio in $\text{Bi}_{1,75-x}\text{Pb}_{0,25}\text{Sb}_x\text{Sr}_2\text{Ca}_2\text{Cu}_3\text{O}_y$ ($0.00 \leq x \leq 0.20$) system

4 Conclusions

In this work, we have studied the influence of substitutional ratio (Sb) on the superconducting and structural properties of $\text{Bi}_{1.75-x}\text{Pb}_{0.25}\text{Sb}_x\text{Sr}_2\text{Ca}_2\text{Cu}_3\text{O}_y$ ceramic superconductor system.

Samples prepared by applying five different substitutional ratio have been characterized by resistivity-temperature determinations, X-ray diffraction patterns, scanning electron microscopy photographs and density measurements were carried out by Archimedes water displacements method. Additional data about properties of the systems were obtained by determining the unit cell parameters by using x-ray diffraction data.

The resistivity-temperature curves is linear up to the onset temperature, in accordance with the metallic character of the samples. Higher T_c value at Sb substitution ratio 0.1 (sample C), and then decrease for further increasing of substitution. Onset temperature for undoped sample was determined as 108 K while for Sb substituted B, C, D, E samples were found respectively as 106, 110, 107, 104 K. Transition temperatures are obtained as 87, 75, 87, 86, 47 K respectively, for all samples A to E. Transition width, a sign of the purity of the system, in A, C, D samples were observed as narrow and in B, E samples as wide. Furthermore double transition temperature were observed in E sample with $x = 0.20$ substitutional ratio.

X-ray diffraction results indicate that the samples have multiphase structure and contain Bi-2212 phase as main phase. The most evident peak which was observed in all samples is L(115) peak. The variation of intensity of this peak with substitutional ratio was investigated. From the EDAX analysis, sample C has maximum oxygen content in the doped samples.

In conclusion, when it was analysed of the results obtained from critical temperatures measurements, XRD analysis, SEM microphotographs, calculated unit cell parameters, it has been shown that the substitution with Sb affect the structure of samples in different manner. Substitution of Sb in Bi sites enhanced the superconducting properties. Sample C has better superconducting properties than the other samples. After this study detailed examination of the nano-sized substitution Sb will be important to understand the contribution of antimony.

References

1. C. Michel, M. Hervieu, M.M. Borel, A. Grandin, F. Deslandes, J. Provost, B. Raveau, *Z.Phys. B* **68**, 421–423 (1987)
2. H. Maeda, Y. Tanaka, M. Fukutomi, T. Asano, *Jpn. J. Appl. Phys.* **27**, L209–L210 (1988)
3. R.M. Hazen, C.T. Prewitt, R.J. Angel, N.L. Ross, L.W. Finger, C.G. Hadjidakos, D.R. Veblen, P.J. Heaney, P.H. Hor, R.L. Meng, Y.Y. Sun, Y.Q. Wang, Y.Y. Xue, Z.J. Huang, L. Gao, J. Bechtold, C.W. Chu, *Phys. Rev. Lett.* **60**, 1174–1177 (1988)
4. J.M. Tarascon, W.R. McKinnon, P. Barboux, D.M. Hwang, B.G. Bagley, L.H. Greene, G.W. Hull, Y. LePage, N. Stoffel, M. Giroud, *Phys. Rev. B* **38**, 8885–8892 (1988)
5. U. Endo, S. Koyama, T. Kawai, *Jpn. J. Appl. Phys.* **27**, L1476–L1479 (1988)
6. S.A. Sunshine, T. Siegrist, L.F. Schneemeyer, D.W. Murphy, R.J. Cava, B. Batlogg, R.B. van Dover, R.M. Fleming, S.H. Glarum, S. Nakahara, R. Farrow, J.J. Krajewski, S.M. Zahurak, J.V. Waszczak, J.H. Marshall, P. Marsh, L.W. Rupp Jr, W.F. Peck, *Phys. Rev. B* **38**, 893–896 (1988)
7. R. Escudero, E. Chavira, D. Rios-Jara, *Appl. Phys. Lett.* **54**, 1576 (1989)
8. T. Ishida, T. Sakuma, T. Sasaki, Y. Kawada, *Jpn. J. Appl. Phys.* **28**, L559–L562 (1989)
9. S. Koyama, U. Endo, T. Kawai, *Jpn. J. Appl. Phys.* **27**, L1861–L1863 (1988)
10. D. Shi, M.S. Boley, J.G. Chen, M. Xu, K. Vandervoort, Y.X. Liao, A. Zangvil, J. Akujieze, C. Segre, *Appl. Phys. Lett.* **55**, 699–701 (1989)
11. L. Pierre, J. Schneck, D. Morin, J.C. Tolédano, J. Primot, C. Daguét, H. Savary, *J. Appl. Phys.* **68**, 2296–2303 (1990)
12. A.W. Sleight, *Acc. Chem. Res.* **28**, 103–108 (1995)
13. R.J. Cava, *J. Am. Ceram. Soc.* **83**, 5–28 (2000)
14. I.H. Gul, M.A. Rehman, M. Ali, A. Maqsood, *Phys. C* **432**, 71–80 (2005)
15. I.H. Gul, M.A. Rehman, A. Maqsood, *Phys. C* **450**, 83–87 (2006)
16. C. Tingzhu, L. Jiang, F. Chengao, Y. Li, L. Yuntao, Z. Guien, M. Zhiqiang, W. Haiqian, C. Zhaojia, Z. Yuheng, *Supercond. Sci. Technol.* **3**, 87–89 (1990)
17. A. Jeremie, K. Alami-Yadri, J.C. Grivel, R. Flükiger, *Supercond. Sci. Technol.* **6**, 730–735 (1993)
18. M. Wang, G. Xiong, X. Tang, Z. Hong, *Phys. C* **210**, 413–416 (1993)
19. F.B. Azzouz, A. M'chirgui, N.N. Slimen, M.B. Salem, *Phys. C* **416**, 115–125 (2004)
20. A.G. Popov, V.P. Dovgopol, F.M. Olevisky, V.S. Melnikov, V.M. Pan, *Supercond. Sci. Technol.* **5**, 654–657 (1992)
21. V. Fruth, M. Popa, A. Ianculescu, M. Stir, S. Preda, G. Aldica, *J. Eur. Ceram. Soc.* **24**, 1827–1830 (2004)
22. Y. Li, S. Kaviraj, A. Berenov, G.K. Perkins, J. Driscoll, A.D. Caplin, G.H. Cao, Q.Z. Ma, B. Wang, L. Wei, Z.X. Zhao, *Phys. C* **355**, 51–58 (2001)
23. M.A. Sekkina, H.A. El-Daly, K.M. Elsabawy, *Supercond. Sci. Technol.* **17**, 93–97 (2004)
24. M.J. Iqbal, R.J. Mehmood, *J. Alloys Compd.* **477**, 386–390 (2009)
25. K. Kocabaş, O. Özkan, Ö. Bilgili, Y. Kadioğlu, H. Yılmaz, *J. Supercond. Nov. Magn.* **23**, 1485–1492 (2010)
26. D. Yazıcı, B. Özçelik, M. Eyüphan Yakıncı, *J. Low Temp. Phys.* **163**, 370–379 (2011)
27. G. Yildirim, S. Bal, E. Yucel, M. Dogruer, M. Akdogan, A. Varilci, C. Terzioglu, *J. Supercond. Nov. Magn.* **25**, 381–390 (2012)
28. A. Arlina, S.A. Halim, M.M. Awang Kechik, S.K. Chen, *J. Supercond. Nov. Magn.* **28**, 1953–1958 (2015)
29. L. Hongbao, Z. Xiaonong, C. Yaozu, Z. Guien, R. Yaozhong, C. Zhaojia, Z. Yuheng, *Phys. C* **156**, 804–806 (1988)
30. L. Hongbao, C. Liezhao, Z. Ling, M. Zhiqiang, L. Xiaoxian, Y. Zhidong, X. Bai, M. Xiangle, Z. Guien, R. Yaozhong, C. Zhaojia, Z. Yuheng, *Solid State Commun.* **69**, 867–868 (1989)
31. J. Heiras, W. Krauss, C. Politis, *Int. J. Mod. Phys. B* **4**, 131–141 (1990)
32. A.G. Popov, V.P. Dovgopol, F.M. Olevisky, V.S. Melnikov, V.M. Pan, *Supercond. Sci. Technol.* **5**, 654–657 (1992)

33. R.Y. Liu, H. Naito, M. Okuda, K. Nakahigashi, Y. Takigawa, T. Matsushita, K. Kurosawa, *Supercond. Sci. Technol.* **5**, 482–488 (1992)
34. N. Kijima, R. Gronsky, *Jpn. J. Appl. Phys.* **31**, L82–L85 (1992)
35. L.R. Motowidlo, P. Haldar, S. Jin, N.D. Spencer, *I.E.E.E. Trans, Appl. Supercond.* **3**, 942–945 (1993)
36. K. Konstantinov, D. Michel, P. Ochin, *J. Mater. Res.* **9**, 2764–2770 (1994)
37. K. Kocabaş, M. Çiftçioğlu, *Phys. Status Solidi* **177**, 539–545 (2000)
38. M.J. Iqbal, R. Mehmood, *Mater. Sci. Eng. B* **135**, 166–171 (2006)
39. H. Azhan, K. Azman, S.Y.S. Yusainee, *Solid State Sci. Technol.* **17**, 215–221 (2009)
40. K. Kocabaş, Ö. Bilgili, N. Yaşar, *J. Supercond. Nov. Magn.* **22**, 643–650 (2009)
41. H. Liu, L. Liu, H. Yu, Y. Zhang, Z. Jin, *J. Mater. Sci.* **33**, 3661 (1998)
42. N.D. Zhigadlo, V.V. Petrashko, Y.A. Semenenko, C. Panagopoulos, J.R. Cooper, E.K.H. Salje, *Phys. C* **299**, 327–337 (1998)
43. S. Bansal, T.K. Bansal, A.K. Jha, R.G. Mendiratta, *Phys. C* **173**, 260–266 (1991)
44. D. Pandey, A.K. Singh, R. Mahesh, V.S. Tiwari, S.K. Kak, *Phys. C* **173**, 476–486 (1991)
45. X. Yang, T.K. Chaki, *Supercond. Sci. Technol.* **6**, 343–348 (1993)
46. J.M. Yoo, K. Mukherjee, *J. Mater. Sci.* **28**, 2361–2365 (1993)
47. S.M. Khalil, *J. Phys. Chem. Solids* **62**, 457–466 (2001)